Revista Mexicana de Astronomía y Astrofísica, **00**, ??–?? (2007)

LONG GAMMA-RAY BURST PROMPT EMISSION PROPERTIES AS A COSMOLOGICAL TOOL

C. Firmani,[1,2] V. Avila-Reese,[2] G. Ghisellini,[1] and G. Ghirlanda[1]

Received 2007 January 11; accepted 2007 February 1

RESUMEN

Se usa una estrecha correlación entre 3 propiedades de la emisión γ de los Estallidos de Rayos Gamma (ERGs) con corrimiento al rojo z conocido (Firmani et al. 2006a) para constreñir parámetros cosmológicos (PCs) en el diagrama de Hubble (DH) con una muestra de 19 ERGs en el amplio rango de $z = 0.17 - 4.5$. El problema de la circularidad se resuelve con un enfoque bayesiano. Encontramos que la cosmología de concordancia ΛCDM es consistente con los datos de los ERGs a nivel de varias pruebas. Si suponemos el modelo Λ, entonces $\Omega_{\rm m}$=$0.31^{+0.09}_{-0.08}$ y Ω_Λ= $0.80^{+0.20}_{-0.30}$ (1σ); el caso plano está dentro del 1σ. Suponiendo planitud, obtenemos $\Omega_{\rm m}$=$0.29^{+0.08}_{-0.06}$, y fijando $\Omega_{\rm m}$=0.28 obtenemos la ecuación de estado de la energía oscura $w = -1.07^{+0.25}_{-0.38}$, estando el caso ΛCDM ($w = -1$) dentro del 1σ. Dado el bajo número de ERGs útiles no se puede aún constreñir bien la evolución de $w = w(z)$, pero encontramos que el caso $w(z) = -1$ (ΛCDM) es consistente al 68.3% CL con los ERGs. Demostramos cómo un amplio rango de z's en la muestra usada (como es el caso de los ERGs) mejora la determinación de los PCs en el DH.

ABSTRACT

Recently, a tight correlation among three quantities that characterize the prompt emission of long Gamma-Ray Bursts (GRBs) with known redshift z, was discovered (Firmani et al. 2006a). We use this correlation to construct the Hubble diagram (HD) with a sample of 19 GRBs in the broad range of $z = 0.17 - 4.5$, and carry out a full statistical analysis to constrain cosmological parameters (CPs). To optimally solve the problem of circularity, a Bayesian approach is applied. The main result is that the concordance ΛCDM cosmology is fully consistent with the GRB data at the level of several tests. If we assume the Λ cosmology, then we find $\Omega_{\rm m}$=$0.31^{+0.09}_{-0.08}$ and Ω_Λ= $0.80^{+0.20}_{-0.30}$ (1σ); the flat-geometry case is within 1σ. Assuming flatness, we find $\Omega_{\rm m}$=$0.29^{+0.08}_{-0.06}$, and fixing $\Omega_{\rm m}$=0.28, we obtain a dark energy equation of state parameter $w = -1.07^{+0.25}_{-0.38}$, i.e. the ΛCDM model ($w = -1$) is within 1σ. Given the low number of usable GRBs we cannot yet constrain well the possible evolution of $w = w(z)$. However, the case $w(z) = -1$ (ΛCDM) is consistent at the 68.3% CL with GRBs. It is shown also how a broad range of z's in the used sample improves the determination of CPs from the HD, which is the case of GRBs as distance indicators.

Key Words: **COSMOLOGICAL PARAMETERS — COSMOLOGY: OBSERVATIONS — DISTANCE SCALE — GAMMA RAYS: BURSTS**

1. INTRODUCTION

The impetuous advance in observational cosmology of the last decade has prompted new challenges for our understanding of the universe and its fate, mainly those related to the nature and physics of the dark energy (hereafter DE) responsible for the current accelerated expansion of the universe. Stimulated by these challenges, the frontiers of physics move now in the direction of exploring new elements

[1]INAF-Osservatorio Astronomico di Brera, Italy.
[2]Instituto de Astronomía, Universidad Nacional Autónoma de México, Mexico.

of high energy physics, the unification of gravity and quantum physics, gravity beyond Einstein relativity, and extra dimensions. At the same time, new astronomical measurements to constrain DE parameters are being developed with the crucial goal of improving quality and reducing systematic uncertainties due to astrophysical effects (e.g. Linder & Huterer 2005). The main task for the new observational studies is to tell us whether DE can be interpreted in terms of either a cosmological constant Λ (the minimal case) or something more complex and changing with time, such as scalar fields. In this endeavor, alternative and complementary methods and experiments are mandatory in order to increase the feasibility and rigor of the results. The use of long gamma-ray bursts (GRBs) as cosmological distance indicators is gaining popularity as a promising method for constraining the cosmological parameters related to the dynamics of the universe. Here we present new advances on this method.

As the most powerful explosions in the universe, long GRBs are of great interest for observational cosmology because they can be detected up to very high redshifts, the current record with spectroscopic determination being GRB 050904 at $z = 6.29$ (Kawai et al. 2006). Ghirlanda, Ghisellini, & Lazzati (2004a) have discovered a tight correlation between the rest frame collimation corrected energy E_γ and the peak energy $E_{\rm pk}$ of the νF_ν prompt emission spectrum for a sample of GRBs with known z. The use of this correlation has proved to be very useful as a method for "standardizing" the GRB energetics and its further application for constructing the Hubble diagram.

The "Ghirlanda" relation has been already used to obtain cosmological constraints, after applying adequate approaches to overcome the problem that, due to the lack of a local (cosmology-independent) calibration, this relation actually depends on the cosmological parameters that we pretend to constrain (Ghirlanda et al. 2004b; Firmani et al. 2005; Xu, Dai, & Liang 2005; Ghirlanda et al. 2006). *As a result, the accelerated expansion of the universe at the present epoch was confirmed independently with GRBs.* Interestingly enough, the marginal inconsistency of the "gold set" of Type-Ia supernovae (SNIa hereafter) with the simple flat-geometry Friedmann-Lemaître-Robertson-Walker (FLRW) cosmology including the cosmological constant (Λ-cosmology) (e.g. Riess et al. 2004; Alam, Sahni, & Starobinsky 2004; Choudhury & Padmanabhan 2004; Jassal, Bagla, & Padmanabhan 2005; Nesseris & Perivolaropoulos 2005b) *is eliminated when the GRB data are added* (Firmani et al. 2005; Ghirlanda et al. 2006).

It is important to stress that GRBs (i) are detected from redshifts much higher than SNIa, and (ii) some degeneracies in determining the cosmological parameters are reduced if the observational sample displays a broad range in redshifts, attaining high values of z (e.g. Weller & Albrecht 2002; Linder & Huterer 2003; Nesseris & Perivolaropoulos 2005a; Ghisellini et al. 2005). In §4 this question will be amply discussed, showing by concrete examples *why a sample broad in redshifts improves the determination of the cosmological parameters.*

The E_γ–$E_{\rm pk}$ relation takes into account the GRB collimation–corrected energy, E_γ=$E_{\rm iso}$(1-cos$\,\theta_{\rm j}$), where $E_{\rm iso}$ is the isotropic–equivalent energy and $\theta_{\rm j}$ is the semi-aperture jet angle. The determination of this angle is model dependent. For the uniform jet model in the standard fireball scenario, $\theta_{\rm j}$ can be determined by the time $t_{\rm break}$when the afterglow light-curve becomes steeper. For a homogeneous circumburst medium $\theta_{\rm j} \propto t_{\rm break}^{3/8}$ (e.g. Sari, Piran, & Halpern 1999), while for a wind circumburst density profile decreasing as r^{-2}, $\theta_{\rm j} \propto t_{\rm break}^{1/4}$ (Nava et al. 2006). Note that to estimate the jet angle from $t_{\rm break}$ one must also assume a specific value of the density of the circumburst material, and the efficiency to convert the fireball kinetic energy into the radiation emitted during the prompt phase. Liang & Zhang (2006; see also Firmani et al. 2006a) found a purely empirical multi-variable correlation among $E_{\rm iso}$, $E_{\rm pk}$ and $t_{\rm break}$ (which is then model-independent and assumption-free). They used this correlation to constrain the cosmological parameters (see also Xu 2005; Ghirlanda et al. 2006).

In Firmani et al. (2006a, hereafter Paper I) we have searched for empirical correlations among $\gamma-$ray prompt quantities alone. In the GRB rest frame the considered quantities were the bolometric corrected $L_{\rm iso}$ and $E_{\rm iso}$, the spectral peak energy $E_{\rm pk}$, and the light-curve variability V and duration $T_{0.45}$ (as defined in Reichart et al. 2001, for more details see § 2 below). In Paper I a ΛCDM cosmology with $\Omega_{\rm m}$=0.3, Ω_Λ=0.7, h=0.7 was assumed to calculate luminosity distances. For the sample of 19 GRBs, for which all the above quantities can be defined, we have found a very tight multi-variable correlation among three quantities, namely $L_{\rm iso} \propto E_{\rm pk}^{1.62} T_{0.45}^{-0.49}$. Within the framework of the fireball scenario, the tightness of the correlation is explained by its scalar nature. We have also estimated the correlation among $E_{\rm iso}$, $E_{\rm pk}$ and $t_{\rm break}$ (Liang & Zhang

2006) for the 15 GRBs with measured $t_{\rm break}$ of our sample, and have proved that the $L_{\rm iso}$–$E_{\rm pk}$–$T_{0.45}$ relation is as tight as the $E_{\rm iso}$–$E_{\rm pk}$–$t_{\rm break}$ one.

Similarly to the "Ghirlanda" (or "Liang & Zhang") correlation, the $L_{\rm iso}$–$E_{\rm pk}$–$T_{0.45}$ correlation can be used as a cosmic ruler for cosmographic purposes. From a practical point of view, the great advantage of the $L_{\rm iso}$–$E_{\rm pk}$–$T_{0.45}$ correlation is that *it involves quantities related only to the $\gamma-$ray prompt emission*. Thus, the establishment of this correlation avoids the need to monitor the afterglow light-curve in order to derive $t_{\rm break}$ which enters both in the "Ghirlanda" and in the "Liang & Zhang" correlation.

In this paper we analyze in detail the cosmographic application of the $L_{\rm iso}$–$E_{\rm pk}$–$T_{0.45}$ relation by using the current dataset. The Hubble diagram is constructed up to redshifts as high as $z = 4.5$. We also describe the Bayesian formalism to solve the 'circularity problem' and compare it with other formalisms. Note that this problem, at least formally, is also present for SNIa samples, as is the case for the recent SN Legacy Survey (Astier et al. 2006). Thus, the Bayesian formalism can also be used to obtain improved cosmological constraints from SNIa samples.

The GRB sample and the $L_{\rm iso}$–$E_{\rm pk}$–$T_{0.45}$ correlation are presented in § 2. The changes of the correlation with cosmology are analyzed in § 3, where we test the robustness of such a correlation for cosmographic purposes. In § 4 we present our approach to parametrize the evolution of DE, and we discuss the degeneracies present in the set of dynamical cosmological parameters We also discuss the Bayesian formalism for solving the circularity problem, comparing it with the conventional χ^2 approach. In § 5 we present the constraints on the parameters that describe the geometry and dynamical evolution of the Universe obtained with the sample of 19 GRBs. The summary and a brief discussion on the current shortcomings and the future of the method presented here are given in § 6.

2. THE SAMPLE AND THE $L_{\rm iso}$–$E_{\rm pk}$–$T_{0.45}$ RELATION

The sample of GRBs with known redshifts and with the necessary observational information available was presented in Paper I. The *rest frame* $L_{\rm iso}$–$E_{\rm pk}$–$T_{0.45}$ correlation presented in Paper I involves:

- the bolometric corrected isotropic energy $E_{\rm iso}$, computed in the rest frame $1 - 10^4$ keV energy range;
- the peak energy $E_{\rm pk}$ of the νF_ν prompt emission time integrated spectrum;
- the time $T_{0.45}$ spanned by the brightest 45% of the total light curve counts above the background and calculated in the 50-300 keV rest frame energy range[3].

In addition to the spectroscopically measured redshift z, the observational data required to estimate $L_{\rm iso}$, $E_{\rm pk}$ and $T_{0.45}$ are the peak flux P, the fluence F, the spectral parameters of a given spectral model (in most cases the Band et al. 1993 model) and the light curve (to estimate $T^{\rm obs}_{0.45}$). The uncertainties in these observables are appropriately propagated to the composite quantities $L_{\rm iso}$, $E_{\rm pk}$ and $T_{0.45}$ under the assumption of no correlation among the measured errors. Note that all the above quantities (except z) are obtained exclusively from the γ-ray prompt emission of the burst.

In Paper I we have used a flat-geometry Λ cosmological model with $\Omega_{\rm m}$=0.3, Ω_Λ=0.7, and h=0.7 to calculate the GRB luminosity distances, $d_{\rm L}$, and to estimate $L_{\rm iso}$. Then, for the 19 GRBs with available observational data a multi-variable regression analysis, *taking into account errors in all the variables*, provided the following best fit:

$$L_{\rm iso} = 10^{52.11\pm0.03}\left(\frac{E_{\rm pk}}{10^{2.37}{\rm keV}}\right)^{1.62\pm0.08}\left(\frac{T_{0.45}}{10^{0.46}{\rm s}}\right)^{-0.49\pm0.07}{\rm erg\ s^{-1}} \quad (1)$$

For a detailed discussion of this correlation, the error estimates, the comparison with other correlations and its interpretation we refer the reader to Paper I.

3. A COSMOLOGICAL TEST FOR THE $L_{\rm iso}$–$E_{\rm pk}$–$T_{0.45}$ CORRELATION

A preliminary cosmological test concerns the sensitivity of the $L_{\rm iso}$–$E_{\rm pk}$–$T_{0.45}$ correlation to the dynamical cosmological parameters. In Paper I we have assumed the currently conventional cosmological model. Now, we will analyze how the correlation and its scatter change from one cosmology to another. For each Λ FLRW cosmology characterized by ($\Omega_{\rm m}$, Ω_Λ) we perform the multiple variable regression analysis on the dataset, using the same method described in Paper I. In this way, the (best fit) $L_{\rm iso}$–$E_{\rm pk}$–$T_{0.45}$ correlation, its relative scatter and the corresponding χ^2_r value for each cosmology

[3] We used the recipe proposed by Reichart et al. (2001) to transform the observed energy range to the rest frame, and the time binning of *HETE–II*, 164-ms (see Paper I).

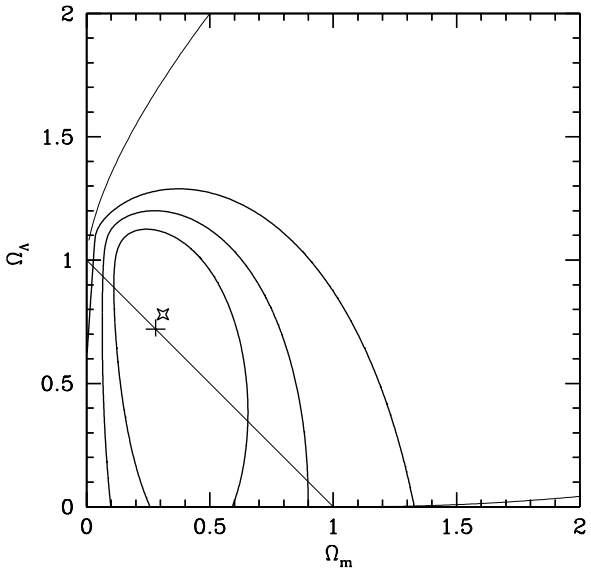

Fig. 1. Contours at 68.3%, 95.5%, and 99.7% CL's obtained by projecting on the ($\Omega_{\rm m}$, Ω_Λ) plane the $L_{\rm iso}$–$E_{\rm pk}$–$T_{0.45}$ relation χ^2_r derived from the fit of the GRB data at each value of the ($\Omega_{\rm m}$, Ω_Λ) pair. The star shows where the χ^2_r reaches its minimum, while the cross indicates the concordance cosmology. This plot shows that the relation $L_{\rm iso}$–$E_{\rm pk}$–$T_{0.45}$ is sensitive to cosmology, so that it may be used to discriminate cosmological parameters if an optimal method to circumvent the circularity problem is used. The diagonal line corresponds to the flat geometry cosmology, the upper curve is the loitering limit between Big Bang and No Big Bang models, and the lower curve indicates the division between accelerating and non-accelerating universes.

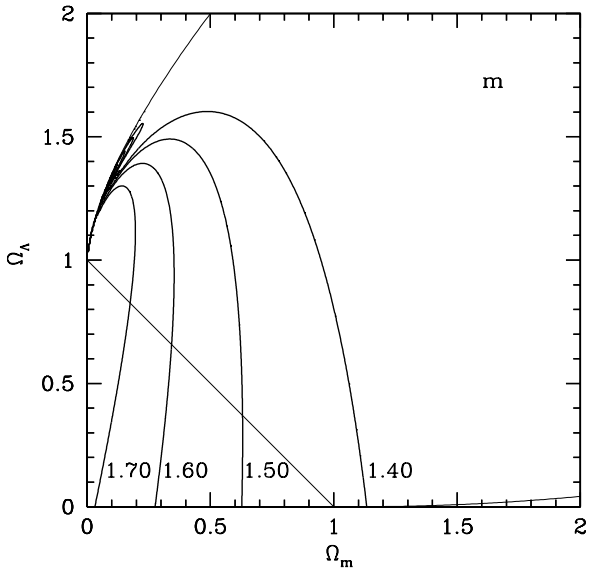

Fig. 2. Contours of constant m in the ($\Omega_{\rm m}$, Ω_Λ) plane. m is the power of $E_{\rm pk}$ in the $L_{\rm iso}$–$E_{\rm pk}$–$T_{0.45}$ relation: $L_{\rm iso} \propto E^m_{\rm pk} T^{-n}_{0.45}$. The other curves in the plot are as in Figure 1.

are obtained and can be used to assign a probability to the ($\Omega_{\rm m}$, Ω_Λ)-pair (Ghirlanda et al. 2004b).

In Figure 1 we show the resulting contours at 68.3%, 95.5%, and 99.7% confidence levels (hereafther CL's), which measure how the χ^2_r (related to the scatter) of the $L_{\rm iso}$–$E_{\rm pk}$–$T_{0.45}$ relation changes with the cosmological parameters. Figure 1 reveals an important sensitivity of the scatter on cosmology and shows the rather surprising result that *the smallest scatter is found for ($\Omega_{\rm m}$, Ω_Λ) = (0.31, 0.78), close to the concordance model ($\Omega_{\rm m}$, Ω_Λ) = (0.28, 0.72) which falls deep inside the 68.3% confidence level region.* This simple and direct ('scatter-scanning') formalism for constraining cosmological parameters does not optimize the use of the available information and is particularly sensitive to the loitering line singularity (Firmani et al. 2005). However, it already shows the potentiality of the $L_{\rm iso}$–$E_{\rm pk}$–$T_{0.45}$ relation for cosmographic purposes. This encourages us to use a more sophisticated formalism in order to obtain more accurate cosmological constraints (see § 4.3).

Figures 2 and 3 illustrate, respectively, how the powers m and n of the $L_{\rm iso}$–$E_{\rm pk}$–$T_{0.45}$ relation ($L_{\rm iso} \propto E^m_{\rm p} T^{-n}_{0.45}$) change, in the ($\Omega_{\rm m}$, Ω_Λ) plane. The lines in Figures 2 and 3 are not to be confused with CL contours on the cosmological parameters. Notice the behavior of the isocontours near the loitering curve, where the dependence of $d_{\rm L}$ on the cosmological parameters becomes singular. The exponents of the $L_{\rm iso}$–$E_{\rm pk}$–$T_{0.45}$ relation do not change dramatically in a wide range of ($\Omega_{\rm m}$, Ω_Λ) values, even if these changes are significantly larger than the small standard deviations of the exponents obtained in the fits (see e.g. Eq. 1). We hope that these results can help for the theoretical interpretation of the obtained correlation, indicating the(rather small) range of the allowed m and n values.

4. CONSTRAINING THE COSMOLOGICAL PARAMETERS IN THE HUBBLE DIAGRAM

4.1. *Cosmological Models with Dark Energy*

The accelerated expansion of the universe is often explained by the dominance in the present-day universe of a self-repulsive medium (DE) with an equation of state parameter $w = p_{\rm DE}/\rho_{\rm DE}c^2 < -1/3$. The simplest interpretation of DE is the homogeneous and inert cosmological constant Λ, with $w = -1$ and $\rho_{\rm DE} = \rho_\Lambda$ =const. The combinations of

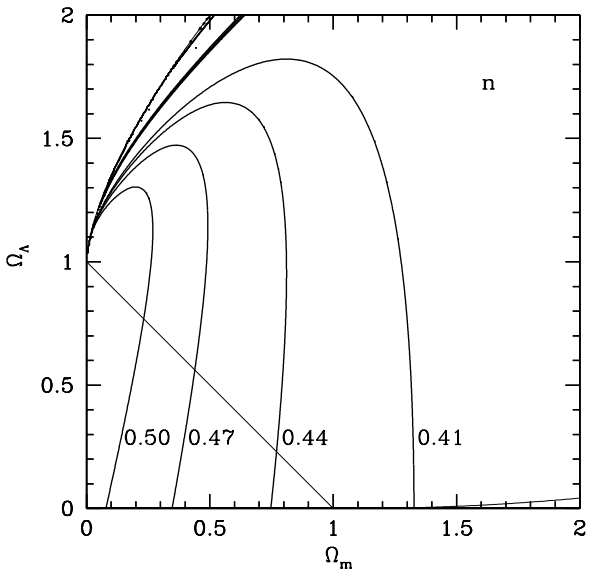

Fig. 3. Contours of constant n in the (Ω_m, Ω_Λ) plane. n is the power of $T_{0.45}$ in the L_{iso}–E_{pk}–$T_{0.45}$ relation: $L_{iso} \propto E_{pk}^{m} T_{0.45}^{-n}$. The other curves in the plot are as in Figure 1.

different cosmological measurements tend to favor models where DE is Λ and (Ω_m, Ω_Λ)$\approx$(0.28, 0.72) (the so-called concordance model, e.g. Spergel et al. 2003; Tegmark et al. 2004; Seljak et al. 2005). Nevertheless, it is important to note that, due to a variety of degeneracies in the parameter space, there are not yet any reliable joint constraints to the complete set of cosmological parameters, even after combining different cosmological probes and data samples (e.g. Bridle et al. 2003). Different probes can even lead to constraints which are not in complete agreement among them (when treated separately), as is the case of *WMAP* observations of the CMB and the "gold set" of Type-Ia SNe (Jassal et al. 2005). Note that a more recent analysis based on the SN Legacy Survey has reduced this apparent discrepancy by favoring the simple flat Λ cosmological model (Astier et al. 2006).

Through samples of "standard candle" objects, such as Type-Ia SNe or GRBs, it is possible to construct the Hubble diagram and, by comparing the data points with the model curves (for different choices of Ω_m and Ω_Λ), to constrain these cosmological parameters. It is clear that, allowing w to have values different from -1, or even evolving, increases the number of free parameters to fit. Up to now, the existing datasets do not allow to fit together all these parameters. The most common approach is to fit only a couple of cosmological parameters, keeping all the others fixed. Such an exercise is in any case important since, for instance, the cosmological constant explanation of DE faces serious theoretical problems (see for reviews e.g. Padmanabhan 2003; Sahni 2004). Therefore, alternative scenarios, where w is different from -1 or even variable with z, have been proposed and extensively investigated.

According to the approach mentioned above, we proceed here in three stages. First, we constrain the two parameters, (Ω_m, Ω_Λ), of the (minimal) Λ cosmology ($w = -1$), and further check whether the concordance model (implying flat geometry) is statistically consistent with the constraints. Next, we generalize to models with w =const (static DE), but assuming a flat geometry in order to have only 2 fitting parameters, Ω_m and w =const. Finally, we generalize to evolving (dynamical) DE models, where w changes with z according to a parametric form, assuming a flat geometry and $\Omega_m = 0.28$. In the two last stages, with some redundancies, we again check whether the concordance model is statistically consistent with the constraints, i.e. whether $w = -1 =$ const is within the 68.3% CL region. For the dynamical DE models, we explore also how much the observational constraints favor the case of an evolving or a static w. Note that any parametrization of $w(z)$ is limited and arbitrary.

To model an evolving DE we use a rather general parametrization for w proposed by Rapetti, Allen, & Weller (2005):

$$w(z) = w_0 + w_1 \frac{z}{z_t + z}, \tag{2}$$

where the parameter w_0 gives the present-day (i.e. at $z = 0$) equation of state; $w_1 = w_\infty - w_0$ gives the increment of w from the present value to $z = \infty$ and z_t is a redshift transition scale. Note that z_t should not be confused with the transition redshift where the expansion goes from decelerating to accelerating). The derivative of $w(z)$ at present is $w_0' = w_1/z_t$. The evolution of the Hubble parameter is given by

$$H^2 = H_0^2 \left[\Omega_m (1+z)^3 + \Omega_\Lambda f(z) + \Omega_k (1+z)^2\right] \tag{3}$$

where $\Omega_k = 1 - \Omega_m - \Omega_{DE}$,

$$f(z) = (1+z)^{3(1+w_\infty)} e^{-3(w_\infty - w_0)g}, \tag{4}$$

and

$$g = \frac{1-a_t}{1-2a_t} \ln\left[\frac{1-a_t}{a(1-2a_t)+a_t}\right], \tag{5}$$

where a is the scale factor and $a_t = 1/(1+z_t)$ is the corresponding transition scale factor.

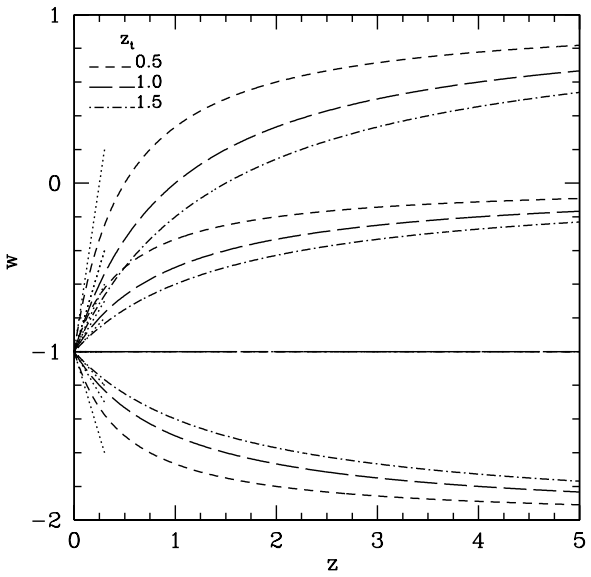

Fig. 4. Dependence of the equation of state parameter w on z as described by Eq. (2). For the plot, w_0=−1 is assumed. Values of w_1=2, 1, 0 and −1 (from top to bottom respectively) and of z_t=0.5, 1.0, and 1.5 (see labels inside the panel) for each w_1 are used. The dotted lines are the tangent lines of each curve at $z = 0$ and represent the linear approximation.

The simple linear approximation commonly used in previous works (e.g. Riess et al. 2004; Firmani et al. 2005), is obtained by making z_t arbitrarily large and assigning a given value to w_0', which in this case is the slope of the $w(z)$ function. The parametrization of Linder (2003) is recovered by setting $z_t = 1$ ($a_t = 1/2$). Figure 4 shows the family of parametric curves given by Eq. (2). Here $w_0 = -1$, $w_1 = -1$, 0, 1 and 2 and $z_t = 0.5$ (short-dashed), 1.0 (long-dashed) and 1.5 (point-dashed). The dotted lines show the linear approximation at present.

Three aspects related to the task of constraining $w(z)$ are worth of mention.

1. Methods based on the construction of the Hubble diagram with a given class of standard candles provide the primary source of information on the evolution of DE [4], which is expected to become dominant only at low redshifts ($\lesssim 1$).

2. If the redshift range of the sources is small, in particular limited to low z's, then the DE parameters and evolution can be constrained only in a limited way (see § 4.2).

3. The constraints on $w(z)$ depend on the (arbitrary) assumed parametrization for $w(z)$. In fact, the space of all possible parametrizations is infinite-dimensional. By choosing "reasonable" parametrizations, both in the physical sense and in that of the limitations of the observational data, the main information we may intend to derive refers only to general aspects such as whether there is evidence or not of DE evolution, and what is the direction of this evolution (e.g. Linder & Huterer 2005). Adequate parametrizations are those with a minimum number of parameters but allowing the widest range of variation of w over the z range in which $w\prime(z)$ is best constrained by the given class of standard candles (Upadhye, Ishak & Steinhardt 2005). For the parametrization of Eq. (2), the smaller is z_t, the larger the allowed change for $w(z)$ at low z's, where observational data are available (see Figure 4).

[4]We notice that besides of the methods based on the luminosity distance–z diagram are also the methods based on the angular diameter distance–z diagram (e.g. the baryonic acoustic oscillations).

4.2. *The Hubble Diagram for High Redshift Objects*

We now discuss some aspects related to the Hubble diagram used to constrain the cosmological parameters. GRBs are the natural objects for extending cosmographic studies up to very high redshifts, and thus for inferring the behavior of DE, in particular, whether and how it evolves. A fundamental issue is, therefore, to understand all the power of the information which can be extracted from using the GRBs as standard candles extending up to very high redshifts. In particular, one should be aware of the several degeneracies (correlations) that appear among the cosmological parameters at different redfshifts.

To study such degeneracies and to understand the shape of the CL's in the parameter space, it is instructive to explore the behavior of the luminosity distance $d_{\rm L}$ at different redshifts z in a given cosmological parameter space. Consider first the Λ cosmology, where the parameters are $\Omega_{\rm m}$ and Ω_Λ. In counterclockwise rotation, the stripes shown in Figure 5 represent the regions of the ($\Omega_{\rm m}$, Ω_Λ) plane where $d_{\rm L}$varies by ± 1% for z = 0.5, 1, 1.5, and 3, respectively, assuming that each stripe passes through the fiducial point ($\Omega_{\rm m}$, Ω_Λ)=(0.33, 0.77) (see below the reasons for this choice).

The stripes in Figure 5 show that the degeneracy (correlation) between $\Omega_{\rm m}$ and Ω_Λ varies with z. This has immediate implications for cosmographic methods based on luminosity distance measurements.

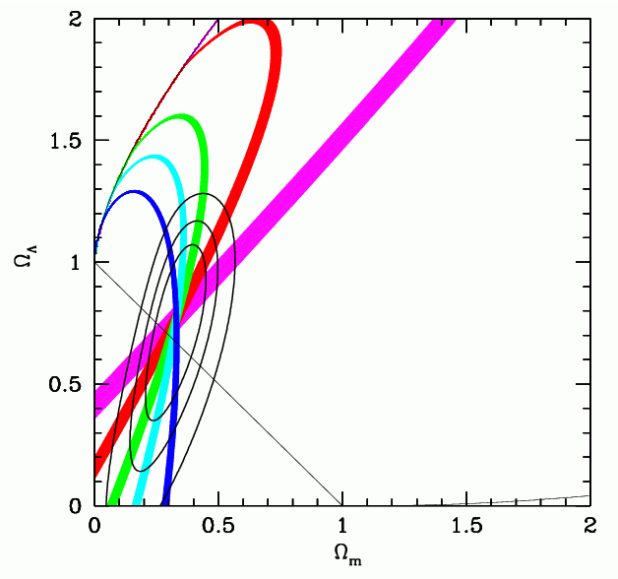

Fig. 5. Regions of ±1% variation around lines of constant d_L in the (Ω_m, Ω_Λ) plane, assuming that each line passes through the fiducial point (Ω_m,Ω_Λ) = (0.33, 0.77). In counterclockwise rotation, the regions are at redshifts 0.5, 1.0, 1.5, 2.0, and 3.0, respectively [in the electronic version of this paper z = 0.5 (magenta), 1.0 (red), 1.5 (green), 2.0 (cyan), and 3.0 (blue)]. This plot illustrates the degeneracy between the parameters Ω_m and Ω_Λ (Λ cosmology) and how this degeneracy does change with z. The ellipses are contours at 68.3%, 95.5%, and 99.7% CL's for the fit to a Λ cosmology from the GRB Hubble diagram, using a L_{iso}–E_{pk}–$T_{0.45}$ relation supposed to be known, and therefore fixed and cosmology-independent (see text for more details). Note that the main orientation of the ellipses is along the "stripes" with $z \approx 1.5$, which corresponds roughly to the typical redshifts of the GRB sample. The other curves in the plot are as in Figure 1.

Taking into account the measurement uncertainties, a specific "standard candle" determines a range of luminosity distances d_L and consequently a stripe on the (Ω_m, Ω_Λ) diagram. For a sample of standard candles characterized by a small range in redshifts, the corresponding CL's in the (Ω_m, Ω_Λ) diagram will be very elongated (high degeneracy) and will have the major axis oriented in the direction of the stripe of the average redshift of the sample. Therefore, a counterclockwise rotation of the CL's is expected when the average redshift of the standard candle sample used to derive the CL's increases. This easily explains why the CL's derived by using SNIa data are elongated and oriented approximately along the direction of the $z \sim 0.6$ stripe (see Figure 8), while the contours derived using our GRB sample, of larger average redshift ($z \sim 1.5$) are more "vertical". Note that, although our GRB sample contains a factor of 10 fewer objects than SNIa, it produces a comparatively narrow contour region, thanks to the broad distribution of redshifts of the GRBs in the sample.

Figure 5 also shows that the width of the stripes (i.e. the uncertainty in (Ω_m, Ω_Λ) associated to a given luminosity distance) decreases for larger z's. This is a consequence of the topology of the surfaces of constant d_L: at low redshift the surface is a gently tilted plane, at high redshifts the surface is more warped, and there appears a "mountain" with a peak close to $\Omega_m \sim 0.0$ and $\Omega_\Lambda \sim 1$. As a consequence, the stripes at high z's are curved, and at very high z's they surround the "mountain peak". Note that, as a consequence of the increasing slope of the d_L surface, the width of the stripes at high redshifts becomes narrower for large Ω_Λ–values.

From Figure 5 we conclude that in order to reduce the degeneracy and improve the accuracy of the constraints of Ω_m and Ω_Λ by using the luminosity distance method, the sample of observed sources should span a range of redshifts as large as possible.

The fiducial point, (Ω_m, Ω_Λ) = (0.33, 0.77), and the CL contours in Figure 5 have been calculated in the following way. We began by using arbitrary trial values for Ω_m and Ω_Λ to define a fiducial (unique) L_{iso}–E_{pk}–$T_{0.45}$ relation. Further, we calculated the χ^2_r's in the whole (Ω_m, Ω_Λ) plane using such fiducial L_{iso}–E_{pk}–$T_{0.45}$ relation to assign the luminous distance to each GRB of known z. If the minimum of the χ^2_r's was smaller than the χ^2_r corresponding to the trial (Ω_m, Ω_Λ) values, then the (Ω_m, Ω_Λ) values corresponding to the minimum χ^2_r were used to define a new fiducial L_{iso}–E_{pk}–$T_{0.45}$ relation in a new iterative step. This procedure was repeated until convergence. The CL's correspond to the 68.3%, 95.5%, and 99.7% (1σ, 2σ and 3σ) probabilities provided by the χ^2 statistics. The procedure should be considered here as a (naive) simulation to constrain Ω_m and Ω_Λ by using a *unique and well calibrated* L_{iso}–E_{pk}–$T_{0.45}$ relation. Interestingly enough, the convergence (Ω_m, Ω_Λ) values in our exercise lie close to those of the concordance cosmology. However, we remark that this procedure is based on incorrect assumptions; it is introduced here only for heuristic reasons.

With an analysis similar to that applied in Figure 1, we also study the behavior of d_L in the diagrams (Ω_m, w=const) and (w_0, w_1) for flat geome-

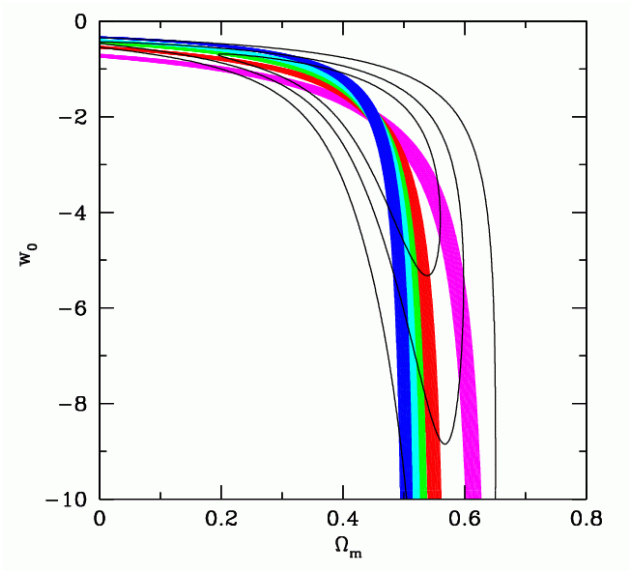

Fig. 6. Same as Figure 5 but in the ($\Omega_{\rm m}$, w) plane for a flat cosmology with static DE. The fiducial point is ($\Omega_{\rm m}$, w) = (0.45, −2.00). Taking the vertical regions of the stripes, the redshifts are 0.5, 1.0, 1.5, 2.0, and 3.0 from right to left, respectively [in the electronic version of this paper $z = 0.5$ (magenta), 1.0 (red), 1.5 (green), 2.0 (cyan), and 3.0 (blue)]. For low values of $\Omega_{\rm m}$, w is almost independent from $\Omega_{\rm m}$, while the opposite happens for high values of $\Omega_{\rm m}$. The dependence of the $\Omega_{\rm m}$–w degeneracy on z is weak. As in Figure 5, the bent ellipses are the contours of CL from the corresponding GRB Hubble diagram, using a $L_{\rm iso}$–$E_{\rm pk}$–$T_{0.45}$ relation supposed to be known, and therefore fixed and cosmology-independent.

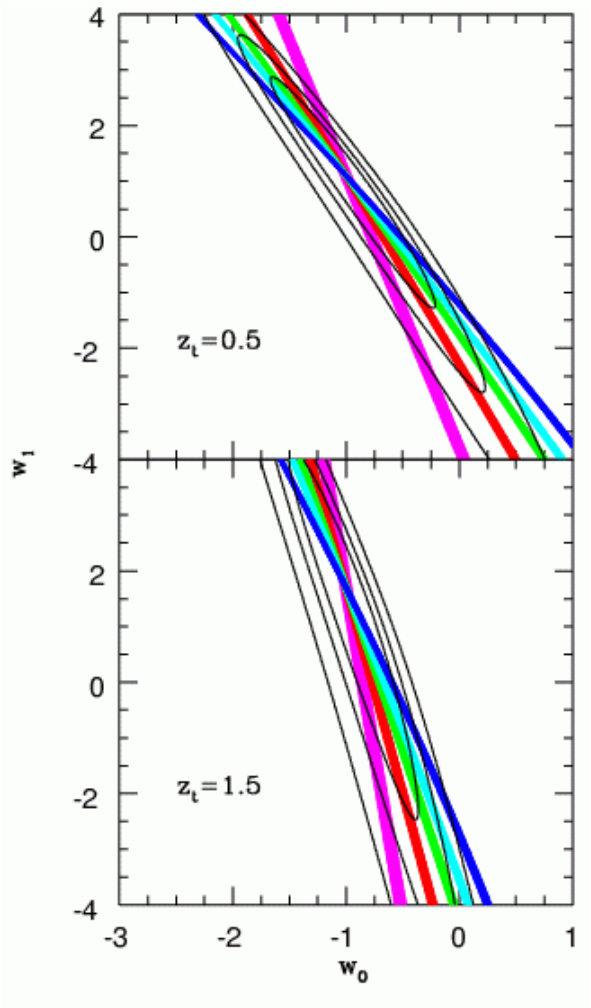

Fig. 7. Same as Figure 5 but in the (w_0, w_1) plane for a flat geometry cosmology with dynamic DE and $\Omega_{\rm m}$= 0.28. The evolving $w(z)$ is parametrized according to Eq. (2) with z_t=0.5 (upper panel) and z_t=1.5 (lower panel). The fiducial points are (w_0, w_1) = (−1.00, 1.08) and (w_0, w_1) = (−1.01, 0.61), respectively. Taking the lower part of the stripes, the redshifts are 0.5, 1.0. 1.5, 2.0 and 3.0 from left to right, respectively [in the electronic version of this paper $z = 0.5$ (magenta), 1.0 (red), 1.5 (green), 2.0 (cyan), and 3.0 (blue)]. As in Figure 5, the ellipses are the contours of CL from the corresponding GRB Hubble diagram, using a $L_{\rm iso}$–$E_{\rm pk}$–$T_{0.45}$ relation supposed to be known, and therefore fixed and cosmology-independent.

try cosmological models. In the latter case, we have further assumed that $\Omega_{\rm m} = 0.28$ and used Eq. 2 with $z_t = 0.5$ and 1.5 to describe the evolving DE. Figures 6 and 7 show the regions of $d_{\rm L}$=const for $z = 0.5, 1, 1.5, 2$, and 3 (see details in the figure captions) assuming in each case that the center of each stripe passes through a given fiducial point.

The fiducial point in each case is [($\Omega_{\rm m}$, w = 0.45, −2.00), (w_0, w_1= −1.00, 1.08) for z_t=0.5, and (w_0, w_1= −1.01, 1.61) for z_t=1.5]. The CL's in the ($\Omega_{\rm m}$, w) and (w_0, w_1) plane, represented in Figure 6 and Figure 7 respectively, were computed following the same procedure described above for the ($\Omega_{\rm m}$, Ω_Λ) plane. The 1σ, 2σ, and 3σ CL's in Figure 6 and 7 were provided by the corresponding χ^2 statistics. Figures 6 and 7 show the degeneracies between w =const and $\Omega_{\rm m}$, and between w_0 and w_1 (for z_t=0.5 and 1.5), and how these degeneracies depend on z.

To summarize: the study of the $d_{\rm L}(z)$ surfaces in the different planes helps us to understand the orientations of the CL regions for different samples of cosmological probes, characterized by different average redshifts. This study makes intuitively clear the need to have probes distributed in a large range of redshifts. This in turns implies that SNIa and GRBs complement each other in a natural way.

4.3. *The Bayesian Formalism*

Now we will explore how the correlation $L_{\rm iso}$–$E_{\rm pk}$–$T_{0.45}$ can be used to constrain cosmological parameters through the Hubble diagram. In the previous section we introduced the concept of a *unique well calibrated* $L_{\rm iso}$–$E_{\rm pk}$–$T_{0.45}$ relation; however, this is not the present case. In fact the $L_{\rm iso}$–$E_{\rm pk}$–$T_{0.45}$ *depends on the assumed cosmology*. Therefore the crucial issue in this undertaking is what has been called the "circularity problem": we attempt to constrain the cosmological parameters using a correlation which is cosmology-dependent. This problem arises because, due to the lack of detected low$-z$ GBRs, the $L_{\rm iso}$–$E_{\rm pk}$–$T_{0.45}$ correlation can not be calibrated at low redshifts, where the flux is not affected by a specific cosmology. Another way to calibrate this kind of correlation is with a sample of high-redshift GRBs in a considerably small redshift bin. Ghirlanda et al. (2006) have calculated that ~ 12 GRBs with $z \in (0.9, 1.1)$ can be used to calibrate the "Ghirlanda" relation with a precision higher than 1%. This number might be reached in a few years of observations mainly due to the fact that the jet break time measurement (which enters in the "Ghirlanda" correlation) requires a time-consuming follow up campaign of the GRB optical/NIR afterglow. We estimate that a similar number of GRBs might also be used to calibrate the $L_{\rm iso}$–$E_{\rm pk}$–$T_{0.45}$ correlation. Fortunately enough, as the latter correlation only relies on prompt emission information, we should expect to collect few tens of GRBs with a low redshift dispersion in a few months, provided that an adequate γ-ray instrument acquires the relevant prompt emission information, namely the light curve and a broad band spectrum.

While waiting for a sample of calibrators, adequate statistical approaches should be used in order to optimally recover cosmographic information from the cosmology-dependent points in the Hubble diagram. The Bayesian formalism presented in Firmani et al. (2005) is currently the most suitable method for this purpose and we apply it here for constraining cosmological parameters by using the $L_{\rm iso}$–$E_{\rm pk}$–$T_{0.45}$ relation. The basic idea of such formalism is to find the best-fitted correlation on each point $\bar{\Omega}$ of the explored cosmological parameter space [for instance $\bar{\Omega} = (\bar{\Omega}_{\rm m}, \bar{\Omega}_\Lambda)$] and to estimate, using such a correlation, the scatter $\chi^2(\Omega, \bar{\Omega})$ on the Hubble diagram for any given cosmology Ω. The conditional probability $P(\Omega|\bar{\Omega})$, inferred from the $\chi^2(\Omega, \bar{\Omega})$ statistics, provides the probability for each Ω given a possible $\bar{\Omega}$-defined correlation. By defining $P'(\bar{\Omega})$ as an arbitrary probability for each $\bar{\Omega}$–defined correlation, the total probability of each Ω, using the Bayes formalism, is given by

$$P(\Omega) = \int P(\Omega|\bar{\Omega}) P'(\bar{\Omega}) d\bar{\Omega}, \qquad (6)$$

where the integral is extended over the available $\bar{\Omega}$ space. Note that from the observations one obtains a correlation for each cosmology. Therefore, $P'(\bar{\Omega})$ is actually the probability of the given cosmology. Consequently such probability is obtained by putting $P'(\Omega) = P(\Omega)$ and solving the integral Eq. (6). It should be noted that in the conventional use of the Bayes approach, P' is handled as a given prior probability. Here, instead, P' and P are just the same probability which is solution of Eq. (6).

An elegant Monte Carlo approach allows us to solve Eq. (6), i.e. to find the probability $P(\Omega)$ from this integral equation. We start by determining the empirical correlation for an arbitrary cosmology Ω_0. The Ω_0-defined correlation is used to calculate on the Hubble diagram the probability distribution $p_0(\Omega|\Omega_0) \propto exp(-\chi^2(\Omega, \Omega_0)/2)$. From this probability, we randomly draw the cosmology Ω_1, which is used to determine again the empirical correlation. Then, with the Ω_1-defined correlation, we calculate a new probability distribution $p_1(\Omega)$ that is averaged with $p_0(\Omega)$. The result is the probability distribution $P_1(\Omega)$. From this probability, a cosmology Ω_2 is randomly drawn and is used to determine again the empirical correlation. Applying this correlation in the Hubble diagram gives a new probability distribution $p_2(\Omega)$. The new probability $p_2(\Omega)$ is averaged with the previous ones, $p_0(\Omega)$ and $p_1(\Omega)$, giving the probability distribution $P_2(\Omega)$. The cycle is repeated until convergence, i.e. until $P_i(\Omega)$ did not change significantly with respect to $P_{i-1}(\Omega)$. The convergence should be fast if the empirical correlation is not too sensitive to cosmology. On the contrary, if the correlation is strongly dependent on cosmology, then convergence cannot be attained with this method. Numerical experiments show that for the $L_{\rm iso}$–$E_{\rm pk}$–$T_{0.45}$ relation, convergence is attained after a few thousands of cycles with a result that is independent of the choice of the initial cosmology Ω_0. By introducing some numerical techniques, the convergence can be attained after hundreds of cycles.

The described formalism is very different from assuming that the correlation is known (*unique and well calibrated*) as done in the previous section. It is also different from scanning *directly* the χ^2 parameter for all points in the Ω plane by minimizing the scatter of the data points around a correlation that is found in the very same Ω point, and

therefore changes from point to point, as we did in § 3. Besides, the Bayesian formalism is less affected than the *direct* method by possible discontinuities, like the loitering line in the $(\Omega_{\rm m}, \Omega_\Lambda)$ plane, and it avoids spurious divergences. With the Bayesian formalism, the observational information, provided by correlations like the $L_{\rm iso}$–$E_{\rm pk}$–$T_{0.45}$ one, is optimally extracted for cosmographic purposes as long as this kind of correlations remain uncalibrated at low z.

It should be remarked that there is no formal and rigorous mathematical method for solving the "circularity problem". However, a comparison of Figures 1 and 8 clearly shows how the constraints improve when one or another formalism is used. Xu et al. (2005) have also shown the much better performance of the Bayesian formalism as compared to the other methods.

Finally, we mention that the Bayesian approach has been also used by us (Firmani et al. 2006b) to constrain cosmological parameters from the Supernova Legacy Survey (SNLS, Astier et al. 2006). The SNLS data are given in such a way that they also require a cosmology-dependent calibration. We have found constraints and CL contours in the $(\Omega_m, \Omega_\Lambda)$ plane similar to those of Astier et al. (2006), who used the direct χ^2 minimization method; if anything, our CL contours were slightly narrower. This shows that our method is working for what it has been designed, namely to optimize the data from quasi-standard candles in the Hubble diagram.

5. RESULTS

In this section we present the results on the cosmological constraints obtained with the Bayesian formalism (§ 4.3) applied to the tight $L_{\rm iso}$–$E_{\rm pk}$–$T_{0.45}$ correlation defined with the 19 long GRBs distributed in redshift to up to 4.5. Following § 4.1, we proceed to constrain only 2 parameters each time. In all the models we fix $h = 0.71$. It should be emphasized that our results represent a first attempt, still using a dataset with few numbers and with a quality of the observational information not yet at the level of SNIa. However, these results allow us to quantify the potentiality of the GRB $L_{\rm iso}$–$E_{\rm pk}$–$T_{0.45}$ correlation as an independent cosmological tool.

For comparison purposes, we will also show the cosmological constraints provided by the SNIa "gold set" (Riess et al. 2004, $z < 1.67$). The latter were derived by using the standard (direct) χ^2-fitting procedure. It is worth to mention that the results on cosmological constraints recently presented by the "Supernova Legacy Survey" group ($z < 1.01$; Astier et al. 2006) show distinct trends that are not shared by the "gold" set (see also Nesseris & Perivolaropoulos 2005b; Firmani et al. 2006b).

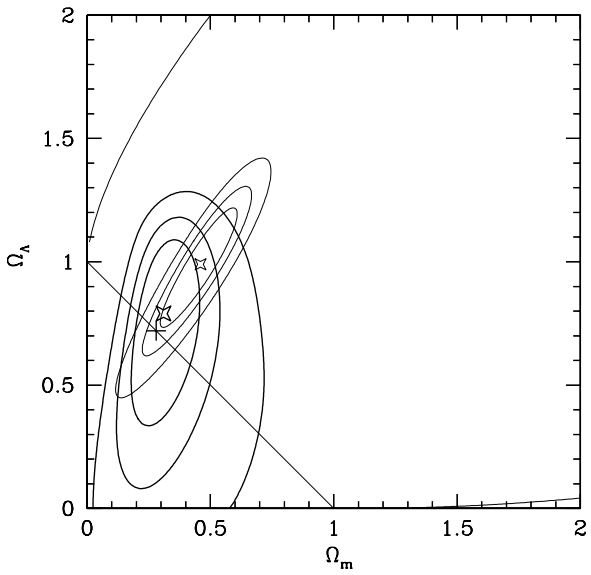

Fig. 8. Constraints on the $(\Omega_{\rm m}, \Omega_\Lambda)$ plane for a Λ cosmology from the GRB Hubble diagram using our Bayesian method to circumvent the circularity problem (thick-line ellipses) and from the "gold set" SNIa Hubble diagram (thin-line ellipses). The ellipses are contours at 68.3%, 95.5%, and 99.7% CL's. The other curves in the plot are as in Figure 1.

5.1. Λ *Cosmology*

In Figure 8 we show the 1σ, 2σ, and 3σ CL's (thick lines) for the $\Omega_{\rm m}$ and Ω_Λ parameters. Notice how the CL's improve with respect to those obtained with the simplest direct χ^2 minimization method used in § 3 (Figure 1). The best-fit cosmology (see the star symbol in Figure 8) corresponds to $\Omega_{\rm m}$=$0.31^{+0.09}_{-0.08}$, Ω_Λ=$0.80^{+0.20}_{-0.30}$ (1σ uncertainty). This result is very close to the flat geometry case. The concordance model is well within the 1σ CL. If the flat geometry case is assumed (i.e. $\Omega_{\rm tot}$= 1), our statistical analysis constrains $\Omega_{\rm m} = 0.29^{+0.08}_{-0.06}$.

The constraints on the Λ cosmology parameters that we obtain with GRBs *alone* are consistent with those obtained through several other cosmological probes (e.g. Hawkins et al. 2003; Schuecker et al. 2003). In turn, this result gives us confidence that GRBs can be used as cosmological probes.

In Figure 8 are also shown the best-fit values (star symbol) and CL regions (thin lines) that we obtain with the SNIa "gold set" (Riess et al. 2004). As these and other authors (e.g. Choudhury &

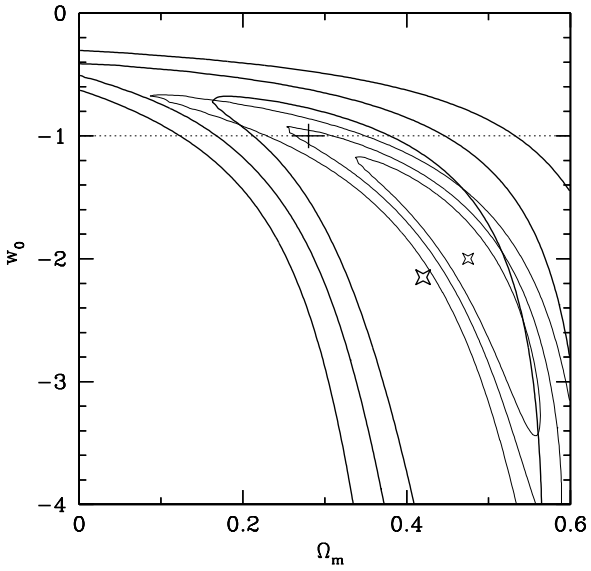

Fig. 9. Constraints on the ($\Omega_{\rm m}$, w) plane for a flat cosmology with static DE from the GRB Hubble diagram using the Bayesian formalism to solve optimally the circularity problem (thick-line ellipses) and from the "gold set" SNIa Hubble diagram (thin-line ellipses). The bent ellipses are contours at 68.3%, 95.5%, and 99.7% CL's.

Padmanabhan 2004; Jassal et al. 2005; Nesseris & Perivolaropoulos 2005b) have shown, the "gold set" provides constraints on $\Omega_{\rm m}$ and Ω_Λ that are only marginally consistent with the concordance model or the *WMAP* CBR constraints.

5.2. *Flat Cosmology with Static (w =const) DE*

Figure 9 shows the 1σ, 2σ, and 3σ CL regions on the ($\Omega_{\rm m}$, w) plane for models with static DE and flat geometry, using the GRB sample (thick lines) and the SNIa "gold set" (thin lines).

The degeneracy here is relevant and higher than the corresponding degeneracy seen in Figure 8. This feature is consistent with the discussion of Figures 5 and 6 of the previous section and has to do with the small rotation of constant $d_{\rm L}$ lines for different redshifts. The reduction of such a degeneracy will be possible by reducing the GRB observational uncertainty as well as by increasing the number of objects (see e.g. Ghirlanda et al. 2006, for a simulation).

The Λ case ($w = -1$) is consistent at the 68.3% CL with the GRB constraints, for values of $\Omega_{\rm m} = 0.29^{+0.08}_{-0.07}$. The concordance model is well inside the 68.3% CL. For a prior $\Omega_{\rm m}$=0.28, we obtain $w = -1.07^{+0.25}_{-0.38}$. Note that the Λ case is not consistent with the SNIa "gold set" at the 68.3% CL.

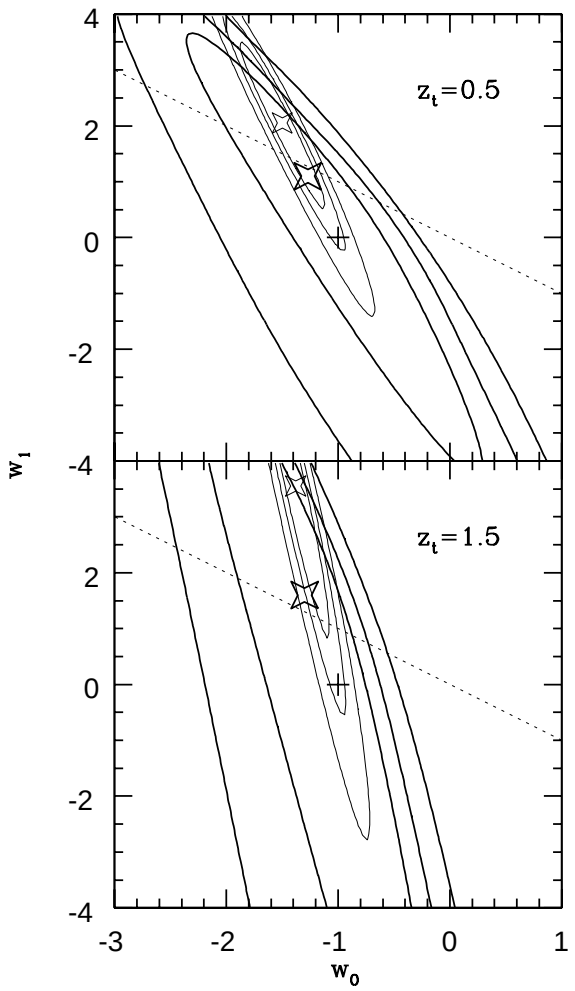

Fig. 10. Constraints on the (w_0,w_1) plane for a flat cosmology with dynamic DE and $\Omega_{\rm m}$=0.28 from the GRB Hubble diagram using the Bayesian formalism to solve optimally the circularity problem (thick-line ellipses) and from the "gold set" SNIa Hubble diagram (thin-line ellipses). Upper and lower panels are for z_t=0.5 and 1.5, respectively. The ellipses are contours at 68.3%, 95.5%, and 99.7% CL's. The diagonal dot-dashed line is the upper limit in the (w_0,w_1)-plane allowed by CMB constraints.

5.3. *Flat Cosmology with Dynamical DE*

Formal constraints on (w_0, w_1) (see Eq. 2), assuming flat-geometry cosmologies (and $\Omega_{\rm m} = 0.28$) with dynamical DE, are presented in Figure 10. Upper and lower panels refer to $z_t = 0.5$ and $z_t = 1.5$, respectively. The thick and the thin line ellipses are the 1σ, 2σ and 3σ CL regions for the GRB and SNIa "gold" samples, respectively. The Λ case (w_0=−1 and w_1=0, which reduces to the concordance model

because of the assumption that $\Omega_{\rm m}$=0.28), is within the 1σ CL.

The typical redshift of our GRB sample is z≈1.5. The best information provided by GRBs on the value of $w(z)$ is expected at the same redshift. Our analysis for $z_t = 0.5$ gives $w(1.5) = -0.5^{+0.7}_{-1.0}$, and for $z_t = 1.5$ it gives $w(1.5) = -0.5^{+0.9}_{-1.9}$. The (still) large uncertainties in the data and the small number of objects do not allow to constrain z_t as a third parameter.

Again, note that the constraints provided by the SNIa "gold set" are not consistent with the concordance model values of w_0 and w_1 at the 68.3% CL.

In general, the "gold" SNIa constraints tend to favor low values of w_0 and large values of w_1, implying (i) a strong evolution of $w(z)$ in the range $0 \lesssim z \lesssim 1$, and (ii) a significant probability for $w(z)$ to cross the $w = -1$ line (phantom divide line, see also e.g. Riess et al. 2004; Alam et al. 2004; Nesseris & Perivolaropoulos 2005b). As reviewed by the last authors, if observations show a significant probability for $w(z)$ to cross the phantom divide line, then all minimally coupled single scalar field models would be ruled out as DE candidates, leaving only models based on extended gravity theories and combinations of multiple fields. It is therefore a key observational task to determine whether $w(z)$ crosses the $w = -1$ line or not. The SNIa "gold set" rejects models that avoid the phantom dividing line at the 1σ CL, while our results with GRBs allow these models (including the concordance one) at the 1σ CL, though the uncertainties for the latter are still much larger than for the former.

Finally, we should emphasize that Eq. (2) is just a mathematical parametrization for the evolution of w, but not a physical model of DE. Although Eq. (2) describes the evolution of w up to any arbitrary large z once its parameters are determined, the changes in w with z suggested by the observational constraints are formally valid only within the redshift range of the observational data. For example, the constraints shown in Figure 10 cannot be used to extrapolate the behavior of $w(z)$ as given by Eq. (2) to z's higher than ~ 3, and ~ 1 for the GRB and SNIa data, respectively.

In fact, at high redshifts there are several observational limits to the values of the parameters of Eq. (2). The most important is related to the CMB anisotropies. The CMB data require $\Omega_{\rm DE} \lesssim 0.1$ at the redshift of recombination, $z = 1100$ (Caldwell & Doran 2004). For the "Rapetti" parametrization that we are using (Eq. [2]) and assuming flat geometry, this condition implies that $w_0 + 0.86 w_1 \lesssim -0.095$, which is close to the general upper limit of $w_\infty = w_1 + w_0 \lesssim 0$ found in the analysis of *WMAP* and other data sets by Rapetti et al. (2005). The dashed line in Figure 10 corresponds to this limit. Interestingly enough, the best-fitting point from the GRB sample in the (w_0, w_1) plane obeys the CMB constraint for $z_t = 0.5$, being slightly out of this constraint for $z_t = 1.5$. Instead, for the SNIa "gold set" the best-fitting points in both cases are far away from the CMB constraint.

6. SUMMARY AND DISCUSSION

Firmani et al. (Paper I) found a very tight correlation among three GRB quantities in their rest frame, $L_{\rm iso}$, $E_{\rm pk}$ and $T_{0.45}$. These quantities were calculated from the $\gamma-$ray prompt emission spectra and light curve, without the addition of any quantity derived from the afterglow, apart from the redshift.

Here we have used this tight correlation to "standardize" the energetics of the currently available sample of 19 GRBs, and to construct an observational Hubble diagram up to the record redshift of $z = 4.5$ and independent from SNIa. Based on the behavior of the luminosity distance as a function of different cosmological parameters (§ 4.2), we have pointed out that samples of standard candles distributed over a wide redshift range are strongly desired for breaking the degeneracy of the cosmological parameters. To overcome the circularity problem that arises due to the lack of a local cosmology-independent calibration of the $L_{\rm iso}$–$E_{\rm pk}$–$T_{0.45}$ relation, we have applied a Bayesian formalism developed in Firmani et al. (2005) and further discussed here. The main results on the cosmological constraints are:

- The $L_{\rm iso}$–$E_{\rm pk}$–$T_{0.45}$ correlation is sensitive to the cosmological parameters of the Λ cosmology (§ 3), having a minimum χ^2_r in ($\Omega_{\rm m}$, Ω_Λ) = (0.31, 0.78), very close to the concordance model (Figure 1).

- For the Λ cosmology, using the Bayesian formalism, the best-fitting values for $\Omega_{\rm m}$ and Ω_Λ are $0.31^{+0.09}_{-0.08}$ and $0.67^{+0.20}_{-0.30}$ (1σ uncertainty), respectively. This result is very close to the flat geometry (Figure 8). The ΛCDM concordance model ($\Omega_{\rm m}$=0.28 and Ω_Λ= 0.72) is well within the 68.3% CL. If one assumes flat geometry, then we find $\Omega_{\rm m} = 0.29^{+0.08}_{-0.06}$.

- For constant w models (static DE) with flat geometry, the Λ case ($w = -1$) is consistent at the 68.3% CL for values of $\Omega_{\rm m} = 0.29^{+0.08}_{-0.07}$.

The ΛCDM concordance model is still within the 68.3% CL.

- For models with dynamical DE, we have parametrized $w(z)$ according to Eq. (2) and used $z_t = 0.5$ and $z_t = 1.5$. Assuming a flat geometry and $\Omega_{\rm m}$=0.28, the Λ case (w_0=−1 and w_1=0, which also in this case corresponds to the concordance model) is again within the 68.3% CL. Interestingly enough, the constraint that the CMB data ($z = 1100$) provide on $w(z)$ as given by Eq. (2) (w_0+0.86$w_1 \lesssim -0.095$), is consistent with the constraints found with GRBs.

We conclude that the different constraints provided by the GRB sample are consistent at the 68.3% CL with the ΛCDM concordance model. This is not the case of the SNIa "gold set". Also, the GRB constraints for flat-geometry models, with DE equation of state parameter either constant or varying with z, are consistent with the constant $w(z)$ case at the 68.3% CL, while the "gold set" SNIe are not. These results show that the GRB method presented here offers already a competitive and reliable way to discriminate cosmological parameters.

The use of the correlation $L_{\rm iso}$–$E_{\rm pk}$–$T_{0.45}$ among prompt γ-ray quantities has proved to be a promising, model-independent and assumption-free method for constructing the observational Hubble diagram up to high redshifts. The accuracy that this correlation provides in constraining cosmological parameters with the current available set of useful GRBs is better than that found with other correlations (either the "Liang & Zhang" correlation or the "Ghirlanda" correlation). Most importantly, the advantage of the $L_{\rm iso}$–$E_{\rm pk}$–$T_{0.45}$ correlation is that it does not involve any quantity related to the afterglow.

Compared to SNIa, the GRB cosmological constraints are less accurate. This is due to the still low number of GRBs having the required data as well as to the relatively large uncertainties associated with these data. However, GRBs provide valuable complementary cosmographic information, in particular due to the fact that GRBs span a much wider redshift distribution than SNIa. As discussed in § 4.2, some degeneracies appear when constraining the cosmological parameters with samples of "standard candles" limited only to low redshifts. The results presented in this paper are a clear proof of the potentiality of using the GRB $L_{\rm iso}$–$E_{\rm pk}$–$T_{0.45}$ relation for cosmographic purposes. After the completion of this paper, a paper by Schaefer (2007), where a combination of several (noisy) empirical correlations of GRBs was used to construct the Hubble diagram up to $z = 6.4$, appeared posted in the arXiv preprint database service. The constraints on the cosmological parameters obtained in that work are similar to ours, though the data and methodology are very different from the ones presented here.

It is worth to mention that as more data of higher quality appear, some assumptions made concerning the cosmographic use of the $L_{\rm iso}$–$E_{\rm pk}$–$T_{0.45}$ relations will either be accepted or refused. For example, in order that this relation be useful for cosmography, it should not evolve, or the way in which it changes with z should be known. It is also important to improve the quality of the data in order to reduce the scatter, as well as to increase the number of usable GRBs. So far, the best physical justification of the $L_{\rm iso}$–$E_{\rm pk}$–$T_{0.45}$ relation derives from its scalar nature, which explains its reduced scatter because it is independent of the relativistic factor Γ (Paper I). A full physical interpretation of this relation is highly desirable, in particular to avoid any uncertainty concerning observational selection effects[5]. However, as an empirical relation used like a distance indicator tool, the main concern is related to reducing the observational scatter. Just recall the case of the famous Tully-Fisher relation for disk galaxies, which has been used as distance indicator for more than twenty years, though until recently its physical foundation was not clear.

Another potential problem for high-redshift GRBs as a cosmological tool is gravitational lensing which systematically brightens distant objects through the magnification bias and increases the dispersion of distance measurements (e.g. Porciani & Madau 2001; Oguri & Takahashi 2006). Recently, Oguri & Takahashi (2006) simulated the gravitational lensing effects on the Hubble diagram constructed with *Swift*-like GRBs following a reasonable luminosity function (Firmani et al. 2004). They showed that lensing bias is not drastic enough to change constraints on dark energy and its evolution. However, they emphasized that the amount of the bias is quite sensitive to the shape of the GRB luminosity function. Thus, an accurate measurement of the luminosity function is important in order to remove the effect of gravitational lensing and to obtain unbiased Hubble diagram.

We finish by emphasizing that the ideal strategy to follow in the future is to combine the SNIa and GRB data sets, and to adopt the same meth-

[5] In a recent paper, appeared after the first submission of the present one, Thompson, Rees & Meszaros (2006) have suggested some interesting hints to understand the origin of the $L_{\rm iso}$–$E_{\rm pk}$–$T_{0.45}$ relation.

ods of handling these data sets of "standard candles" in order to construct their joint Hubble diagram, and thus constrain the cosmological parameters. Of course, the dominant information will be that of SNIa (they outnumber GRBs and the uncertainties on their luminosity are smaller than for GRBs), but GRBs provide valuable information at high redshifts which helps to partially overcome parameter degeneracies and biases. This program is carried out elsewhere (Firmani et al. 2006b).

We thank Giuseppe Malaspina for technical support, and Jana Benda for grammar corrections. We are grateful to the anonymous referee for a through and constructive report that helped to improve the content of the paper. VA-R. gratefully acknowledges the hospitality extended by Osservatorio Astronomico di Brera. This work was supported by PAPIIT-UNAM grant IN107706-3 and by the Italian INAF MIUR (Cofin grant 2003020775_002).

REFERENCES

Alam, U., Sahni, V., & Starobinsky, A. A. 2004, J. Cosmol. Astropart. Phys., 06, 008
Astier, P., et al. 2006, A&A, 447, 31
Band, D., et al. 1993, ApJ, 413, 281
Bridle, S. L., Lahav, O., Ostriker, J. P., & Steinhardt, P. J. 2003, Science, 299, 1532
Caldwell, R. R., & Doran, M. 2004, Phys. Rev. D, 69, 103517
Choudhury, T. R., & Padmanabhan, T. 2004, A&A, 429, 807
Firmani, C., Avila-Reese, V., Ghisellini, G., & Tutukov, A. V. 2004, ApJ, 611, 1033
Firmani, C., Ghisellini, G., Ghirlanda, G., & Avila-Reese, V. 2005, MNRAS, 360, L1
Firmani, C., Ghisellini, G., Avila-Reese, V., & Ghirlanda, G. 2006a, MNRAS, 370, 185 (Paper I)
Firmani, C., Avila-Reese, V., Ghisellini, G., & Ghirlanda, G., 2006b, MNRAS, 372, L28
Ghirlanda, G., Ghisellini, G., Firmani, C., Nava, L., & Tavecchio, F. 2006, A&A, 452, 839
Ghirlanda, G., Ghisellini, G., & Lazzati, D. 2004a, ApJ, 616, 331
Ghirlanda, G., Ghisellini, G., Lazzati, D., & Firmani, C. 2004b, ApJ, 613, L13
Ghisellini, G., Ghirlanda, G., Firmani, C., Lazzati, D., & Avila-Reese, V. 2005, Il Nuovo Cimento C, 28, 639
Hawkins, E., et al. 2003, MNRAS, 346, 78
Jassal, H. K., Bagla, J. S., & Padmanabhan, T. 2005, Phys. Rev. D, 72, 103503
Kawai, N., et al. 2006, Nature, 440, 184
Liang, E., & Zhang, B. 2006, ApJ, 633, 611
Linder, E. V. 2003, Phys. Rev. Lett., 90, 091301
Linder, E. V., & Huterer, D. 2003, Phys. Rev. D, 67, 081303
_____. 2005, Phys. Rev. D, 72, 043509
Nava, L., Ghisellini, G., Ghirlanda, G., Tavecchio, F., & Firmani, C. 2006, A&A, 450, 471
Nesseris, S., & Perivolaropoulos, L. 2005a, J. Cosmol. Astropart. Phys., 10, 001
_____. 2005b, Phys. Rev. D, 72, 123519
Oguri, M., & Takahashi, K. 2006, Phys. Rev. D, 73, 123002
Padmanabhan, T. 2003, Phys. Rep., 380, 235
Porciani, C., & Madau, P. 2001, ApJ, 548, 522
Rapetti, D., Allen, S. W., & Weller, J. 2005, MNRAS, 360, 555
Reichart, D., Lamb, D. Q., Fenimore, E. E., Ramirez-Ruiz, E., Cline, Th. L., & Hurley, K. 2001, ApJ, 552, 57
Riess, A. G., et al. 2004, ApJ, 607, 665
Sahni, V. 2004, Lect. Notes Phys., 653, 141
Sari, R., Piran, T., & Halpern, J. P. 1999, ApJ, 519, L17
Schaefer, B. E. 2007, ApJ, in press (astro-ph/0612285)
Schuecker, P., Caldwell, R. R., Böohringer, H., Collins, C. A., Guzzo, L., & Weinberg, N. 2003, A&A, 402, 53
Seljak, U., et al. 2005, Phys. Rev. D, 71, 103515
Spergel, D. N., et al. 2003, ApJS, 148, 175
Tegmark, M., et al. 2004, Phys. Rev. D, 69, 103501
Thompson, C., Rees, M. J., & Meszaros, P. 2006, ApJ, submitted (astro-ph/0608282)
Upadhye, A., Ishak, M., & Steinhardt, P. J. 2005, Phys. Rev. D, 72, 063501
Weller, J., & Albrecht, A. 2002, Phys. Rev. D, 65, 103512
Xu, D. 2005, preprint (astro-ph/0504052)
Xu, D., Dai, Z. G., & Liang, E. W. 2005, ApJ, 633, 603

V. Avila-Reese: Instituto de Astronomía, Universidad Nacional Autónoma de México, Apdo. Postal 70-264, 04510 México, D. F., Mexico (avila@astroscu.unam.mx).
C. Firmani: INAF-Osservatorio Astronomico di Brera, via E. Bianchi 46, I-23807 Merate, Italy and Instituto de Astronomía, Universidad Nacional Autónoma de México, Apdo. Postal 70-264, 04510 México, D. F., Mexico (firmani@merate.mi.astro.it).
Giancarlo Ghirlanda and Gabrielle Ghisellini: INAF-Osservatorio Astronomico di Brera, via E. Bianchi 46, I-23807 Merate, Italy (giancarlo.ghirlanda, gabriele.ghisellini@brera.inaf.it).